Acta Mechanica Solida Sinica, Vol. 29, No. 1, February, 2016 ISSN 0894-9166
Published by AMSS Press, Wuhan, China

A Comparison of Deterministic, Reliability-Based Topology Optimization under Uncertainties**

Qinghai Zhao[1] **Xiaokai Chen**[1*] **Zhengdong Ma**[2] **Yi Lin**[3]

([1] *Collaborative Innovation Center of Electric Vehicles in Beijing, School of Mechanical Engineering, Beijing Institute of Technology, Beijing,* 100081*, China*)
([2] *Department of Mechanical Engineering, University of Michigan, MI* 48105*, USA*)
([3] *Beijing Automotive Technology Center, Beijing* 100081*, China*)

Received 26 August 2014, revision received 29 October 2015

ABSTRACT Reliability and optimization are two key elements for structural design. The reliability-based topology optimization (RBTO) is a powerful and promising methodology for finding the optimum topologies with the uncertainties being explicitly considered, typically manifested by the use of reliability constraints. Generally, a direct integration of reliability concept and topology optimization may lead to computational difficulties. In view of this fact, three methodologies have been presented in this study, including the double-loop approach (the performance measure approach, PMA) and the decoupled approaches (the so-called Hybrid method and the sequential optimization and reliability assessment, SORA). For reliability analysis, the stochastic response surface method (SRSM) was applied, combining with the design of experiments generated by the sparse grid method, which has been proven as an effective and special discretization technique. The methodologies were investigated with three numerical examples considering the uncertainties including material properties and external loads. The optimal topologies obtained using the deterministic, RBTOs were compared with one another; and useful conclusions regarding validity, accuracy and efficiency were drawn.

KEY WORDS reliability-based design optimization, topology optimization, first-order reliability method (FORM), stochastic response surface method, sparse grid method

I. Introduction

Since the epoch-making work of Bendsøe and Kikuchi[1], a considerable development of continuous structural topology optimization has been seen in both theories and industrial applications during the last two decades, mainly featured by obtaining a material or design parameter distribution within a fixed design domain that minimize/maximize the required objective function while satisfying the given constraint[2,3]. Traditionally, the optimization process was performed in a deterministic manner, where the optimal solution was usually located at the limits of constraint boundaries. However, in the real-life of practical engineering design, variations can inevitably exist in geometric and material properties as well as external loads due to the inherent uncertainty of nature. Therefore, the deterministic topology optimization (DTO) design, without considering such input uncertainties, may not reasonably represent

* Corresponding author. E-mail: chenxiaokai@263.net
** Project supported by the National Natural Science Foundation of China (Nos. 51275040 and 50905017), and the Programme of Introducing Talents of Discipline to Universities (No. B12022). The authors are also grateful to Krister Svanberg for providing his implementation of the MMA algorithm.

the reliability level. For this reason, the reliability-based topology optimization (RBTO) has emerged, by means of which, optimal topologies can be achieved with the effects of uncertainties explicitly taken into account through reliability constraints.

In general, the traditional RBTO techniques are referred to as double-loop (or nest-loop) approaches, where the reliability constraints are transformed, so that the measurable reliability index optimization problems can be solved by using the first-order reliability method (FORM). Two of the most popular FORM-based approaches are the reliability index approach (RIA) and its inverse, the more efficient performance measure approach (PMA)[4]. Maute and Frangopol[5] presented an RBTO framework that combined material-based topology optimization and the PMA for MEMS mechanism design to take into account the uncertainty parameters. Kim et al.[6] formulated the RBTO problems based on the FORM, where the RIA and PMA were compared with each other. The results clearly showed that the PMA had better convergence and efficiency than the RIA. Cho et al.[7] proposed an RBTO procedure for the electro-thermal-compliant mechanism design, where the probabilistic constraints were evaluated by the PMA. However, empirical evidence showed that such double-loop approaches led to substantially high computational cost and weak convergence stability, especially when repeated evaluations of the limit state function are involved in the virtual simulation models for different sets of design and random variables in each design iteration. To overcome these problems, different methods aimed at simplified and efficient formulations have been proposed for solving the RBTO problems. Kharmanda and Olhoff[8] proposed the so-called hybrid (or concurrent) RBTO method, which was based on the simultaneous solution of the reliability and the design optimization problems. The major advantage of this methodology was that it found the global solution in a more efficient way, i.e. without additional computing cost of the reliability evaluation. Mariana et al.[9] performed component and system RBTO using a variant of the single loop method, which was amenable to be compatible with the existing topology optimization software and suitable for practical applications. Nguyen et al.[10] proposed a single-loop algorithm for system reliability-based topology optimization (SRBTO), in which the statistical dependence between limit states was taken into account through the computation of system failure probability using the matrix-based system reliability (MSR) method.

Application of the FORM-based approach can only be possible when the limit state function is known. However, in many practical complex structures, the implicit relationships between the output responses and the input data are difficult to be formulated. To overcome this difficulty, these implicit models were replaced with explicit approximate functions formulated using the meta-modeling techniques based on design of experiments (DOE). Yoo et al.[11] applied traditional response surface method (RSM) and standard response surface method to construct the limit state function in RBTO. Eom et al.[12] extended the use of standard RSM to three-dimensional structure design during the RBTO procedure, where the central composite design (CCD) was used in DOE. It was well recognized that the reliability analysis could be easily implemented when the RSM was applied to construct the limit state function. However, the RSM cannot be applied in the FORM directly, because the input uncertainties are random parameters instead of standard random variables.

Based upon the summary of reported works, in this study, three typical RBTO methodologies were presented, implemented and tested on three numerical examples. The method of solid isotropic microstructure with penalty (SIMP) was used here for topology optimization. To evaluate the probabilistic constraint, the FORM was employed to consider the uncertainties of material properties and external loads. The limit state function was constructed by the stochastic response surface method (SRSM) based on the DOE generated by using the sparse grid method, which was proven as an effective and special discretization technique.

The paper is organized as follows. In §II, topology optimization formulations are presented, including the deterministic topology optimization and the reliability-based topology optimization. The selected three methodologies covering the double-loop formulations (PMA) and the efficient decoupled approaches (Hybrid and SORA) are briefly discussed in §III, respectively. This is followed by a description of the SRSM and the sparse grid method in §IV. The numerical results and discussion on the design are presented in §V. Finally, the conclusion and summary are provided in §VI.

II. Topology Optimization Formulations

2.1. Deterministic topology optimization (DTO)

In topology optimization of continuum structures, many different solution procedures have been developed, such as the homogenization method[13], solid isotropic microstructure with penalty (SIMP)[14], bidirectional evolutionary structural optimization (BESO)[15], and level set method (LSM)[16]. For a detailed review on these methods, the readers are referred to the paper by Eschenauer and Olhoff[17]. In this paper, based on the SIMP, a typical formulation of DTO can be stated as

$$\begin{aligned} &\min_{\boldsymbol{\rho}}: \ C(\boldsymbol{\rho}) \\ &s.t.: \ \begin{cases} G_i(\boldsymbol{\rho}) \geq 0 \quad (i = 1, \dots, m) \\ \boldsymbol{\rho}_{\min} \leq \boldsymbol{\rho} \leq \boldsymbol{\rho}_{\max} \end{cases} \end{aligned} \tag{1}$$

where $\boldsymbol{\rho}$ is the vector of design variables (i.e. the element densities) with upper bounds $\boldsymbol{\rho}_{\max}$ and lower bounds $\boldsymbol{\rho}_{\min}$; C is the objective function (i.e. volume fraction); G_i is the ith constraint function (i.e. structural compliance); and m is the number of constraints.

2.2. Reliability-based topology optimization (RBTO)

In RBTO, the effects of uncertainty can be explicitly characterized by the reliability constraints. Here, two types of variables are involved, i.e. design variables $\boldsymbol{\rho}$ and random variables $\boldsymbol{X}$. A typical RBTO formulation is expressed as

$$\begin{aligned} &\min_{\boldsymbol{\rho}}: \ C(\boldsymbol{\rho}) \\ &s.t.: \ \begin{cases} \Pr\left[G_i(\boldsymbol{\rho}, \boldsymbol{X}) \leq 0\right] \leq P_{f_i}^T \quad (i = 1, \dots, m) \\ \boldsymbol{\rho}_{\min} \leq \boldsymbol{\rho} \leq \boldsymbol{\rho}_{\max} \end{cases} \end{aligned} \tag{2}$$

where $\boldsymbol{X}$ is the vector of random variables (i.e. loads and material properties) with the realizations noted as $\boldsymbol{x}$, identified by probability distributions; G_i is known as the ith limit state function or performance function; $\Pr[\cdot]$ is the probability operator; P_{fi}^T is the admissible failure probability of the ith constraint. It should be noted that the design variables $\boldsymbol{\rho}$ are independent deterministic variables. To evaluate the failure probability with respect to a chosen failure scenario, the failure region is defined as $G(\boldsymbol{\rho}, \boldsymbol{X}) < 0$, and the limit state function as $G(\boldsymbol{\rho}, \boldsymbol{X}) = 0$. The failure probability P_{fi} for each constraint may be obtained by evaluating the following integral:

$$P_{f_i} = \Pr\left[G_i(\boldsymbol{\rho}, \boldsymbol{X}) \leq 0\right] = \int \cdots \int_{G_i(\boldsymbol{\rho}, \boldsymbol{X}) \leq 0} f_{\boldsymbol{X}}(\boldsymbol{x}) \, \mathrm{d}\boldsymbol{x} \tag{3}$$

where $f_{\boldsymbol{X}}(\boldsymbol{x})$ is the joint probability density function (PDF) of random vector $\boldsymbol{X}$. In practice, it is generally difficult or even impossible to obtain the above multidimensional integration, because the limit state functions are sometimes provided in implicit or high nonlinear forms, even without any essential information on the joint density function. Various analytical methods suitable for solving this integral approximately were reviewed by Lee and Chen[18]. Among these approaches, the FORM is a particularly favorable one because of its simplicity and efficiency. The idea of the FORM is that it transforms the integral in the original random space into a measurable reliability index that is interpreted as the minimum distance from the origin to the limit state function in the normalized space (u-space) with the most probable point (MPP) being searched, as shown in Fig.1.

Using the FORM approximation, the failure probability and the allowable failure probability are evaluated by

$$P_{f_i} \approx \Phi(-\beta_i) \quad \text{and} \quad P_{f_i}^T \approx \Phi\left(-\beta_i^T\right) \tag{4}$$

where Φ is the standard cumulative distribution function (CDF); β_i^T is the target reliability index for the ith constraint; and β_i is the reliability index evaluated by the distance from the origin to the MPP in the normalized space[19]. By applying the Rosenblatt[20] or the Nataf transformations[21], random vector $\boldsymbol{X}$ is transformed into an independent and normalized vector $\boldsymbol{U}$ (zero means, unit variance), expressed as $\boldsymbol{U} = \boldsymbol{T}(\boldsymbol{X})$, or $\boldsymbol{X} = \boldsymbol{T}^{-1}(\boldsymbol{U})$. In the case of a normal distribution, a normalized vector $\boldsymbol{U}$ is given by

$$\boldsymbol{U} = \frac{\boldsymbol{X} - \boldsymbol{\mu}_x}{\boldsymbol{\sigma}_x} \tag{5}$$

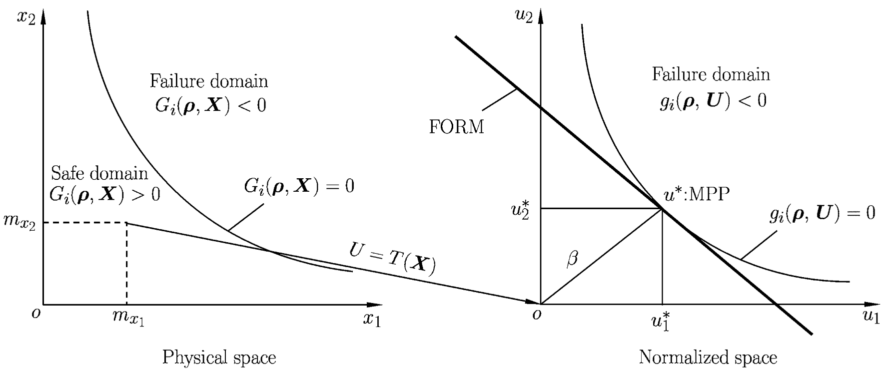

Fig. 1. The first order reliability method (FORM).

where $\boldsymbol{\mu}_x$ and $\boldsymbol{\sigma}_x$ are the vector of mean values and the standard deviations associated with $\boldsymbol{X}$, respectively. Based on the above transformation, the constraint function is further defined as

$$G_i\left(\boldsymbol{\rho}, \boldsymbol{X}\right) = G_i\left(\boldsymbol{\rho}, \boldsymbol{T}^{-1}\left(\boldsymbol{U}\right)\right) = g_i\left(\boldsymbol{\rho}, \boldsymbol{U}\right) \tag{6}$$

where g_i is the ith constraint in the normalized space.

III. Three Approaches for RBTO

3.1. Double-loop RBTO approach

The traditional solution of RBTO problem requires a double-loop iteration, with the outer loop being an optimization problem in terms of the design variables $\boldsymbol{\rho}$, and the inner loop a reliability analysis in terms of the random variables $\boldsymbol{X}$. The two most popular double-loop RBTO approaches are the RIA and its inverse, the PMA. The PMA seems to be robust and efficient, since it is easier to optimize a complex objective function subject to a simple constraint (PMA) than to optimize a simple objective function subject to a complex constraint (RIA)[22].

By using the PMA formulation, the RBTO is expressed as

$$\begin{aligned} &\min_{\boldsymbol{\rho}}: \ C\left(\boldsymbol{\rho}^{(k)}\right) \\ &s.t.: \ \begin{cases} G_i^p\left(\boldsymbol{\rho}^{(k)}, \boldsymbol{x}_i^{(k-1)}\right) \geq 0 \quad (i = 1, \ldots, m) \\ \boldsymbol{\rho}_{\min} \leq \boldsymbol{\rho}^{(k)} \leq \boldsymbol{\rho}_{\max} \end{cases} \end{aligned} \tag{7}$$

where k indicates the current cycle; G_i^p is the target performance with respect to the ith limit state function calculated at the MPP noted as $\boldsymbol{x}_i^{(k-1)}$ in the physical space, given by the transformation of $\boldsymbol{u}_i^{*(k-1)}$. By applying the probabilistic transformation, the MPP $\boldsymbol{u}_i^{*(k-1)}$ is evaluated by the inverse reliability analysis in normalized space, given as

$$\begin{aligned} &\min_{\boldsymbol{u}}: \ g_i\left(\boldsymbol{\rho}^{(k-1)}, \boldsymbol{u}\right) \\ &s.t.: \ \|\boldsymbol{u}\| = \sqrt{\boldsymbol{u}^{\mathrm{T}}\boldsymbol{u}} = \beta_i^T \end{aligned} \tag{8}$$

This is a special optimization problem with the spherical-equality constraint. Besides using the general-purpose mathematical programming algorithms, the problem can be solved by some high-efficient algorithms, such as the methods of the so-called advanced mean value (AMV), the conjugate mean value (CMV), and the hybrid mean values (HMV). Brief overviews on such methods were presented by Wu[23] and Grujicic[24]. The AMV method is formulated, here, simply defined as

$$\boldsymbol{u}^{(0)} = 0 \quad \text{and} \quad \boldsymbol{u}^{(k+1)} = -\beta_i^T \frac{\nabla_u g_i\left(\boldsymbol{u}^{(k)}\right)}{\left\|\nabla_u g_i\left(\boldsymbol{u}^{(k)}\right)\right\|} \tag{9}$$

where $\nabla_u g_i\left(\boldsymbol{u}^{(k)}\right) = \left\{\dfrac{\partial g_i}{\partial u_1}, \dfrac{\partial g_i}{\partial u_2}, \cdots, \dfrac{\partial g_i}{\partial u_n}\right\}^{\mathrm{T}}\Bigg|_{\boldsymbol{u}^{(k)}}$.

Applications of the RBTO with double-loop procedure is restricted due to the high numerical cost, especially when virtual simulation models (e.g. the finite element models) are involved.

3.2. Decoupled RBTO approaches

The main idea of decoupled techniques is to convert the RBTO into a sequence of deterministic topology optimization and independent reliability analysis. By means of these approaches, the reliability analysis is not carried out within the topology optimization loop, but before/after the topology optimization procedure. Therefore, the computational efficiency is improved significantly and the design is generally updated from cycle to cycle until the convergence criterion is achieved.

3.2.1. Hybrid (or concurrent) method for RBTO

This approach was initiated by Kharmanda et al.[8], which consists of a sequence of beforehand reliability analyses and deterministic topology optimization. At first, the chosen random variables are modified as deterministic quantities according to the MPP obtained from the reliability index evaluation and sensitivity analysis for the objective function with respect to the variables. Finally, using the resulting random variables, the new reliable and optimal topology is obtained through the deterministic topology optimization process. The so-called hybrid (or concurrent) RBTO method can be expressed as

$$\begin{aligned} & given: \quad \boldsymbol{x}_i \quad (i=1,\cdots,m) \\ & \min_{\boldsymbol{\rho}}: \ C(\boldsymbol{\rho}) \\ & s.t.: \ \begin{cases} G_i(\boldsymbol{\rho}) \geq 0 \quad (i=1,\ldots,m) \\ \boldsymbol{\rho}_{\min} \leq \boldsymbol{\rho} \leq \boldsymbol{\rho}_{\max} \end{cases} \end{aligned} \tag{10}$$

where $\boldsymbol{x}_i$ is the MPP vector for the chosen random variables in the physical space with respect to the ith limit state given by the transformation of normalized variables u_i^T, obtained from the reliability index evaluation, given as

$$\begin{aligned} & \min_{\boldsymbol{u}} \ \ \|\boldsymbol{u}\| = \beta_i = \sqrt{\sum u_j^2} \quad (j=1,\ldots,n) \\ & s.t.: \ \beta_i(\boldsymbol{u}) \geq \beta_i^T \end{aligned} \tag{11}$$

where n is the number of random variables with respect to the ith limit state function. Derivative of the reliability index β_i with respect to the normalized variable u_j can be analytically provided by

$$\frac{\partial \beta_i}{\partial u_j} = \frac{1}{2}\left(\sum u_j^2\right)^{-1/2} \cdot 2u_j = \frac{u_j}{\beta_i} \tag{12}$$

In the case of normal distribution, the resulting random variable x_j is conveniently transformed by using Eq.(5), where the normalized variable u_j has the same sign with the corresponding gradient.

$$x_j = m_{x_j} + \operatorname{sign}\left(\frac{\partial C}{\partial m_{x_j}}\right) u_j \sigma_{x_j} \tag{13}$$

where m_{x_j} and σ_{x_j} are the mean value and standard-deviation for the jth random variable, respectively. Sensitivity of the objective function with respect to the chosen means of random variables can be simply calculated using the classical finite difference approach, written as

$$\frac{\partial C}{\partial m_{x_i}} = \frac{\Delta C}{\Delta m_{x_i}} = \frac{C(m_{x_i} + \Delta m_{x_i}) - C(m_{x_i})}{\Delta m_{x_i}} \tag{14}$$

where Δm_{x_j} is the difference step, usually assigned as Δm_{x_j}=0.01m_{x_j}. The main advantage of this new RBTO model lies in that the resulting optimal topologies are more reliable and different than the deterministic topologies when subject to different target reliability levels. It is noted that the limit state function is a linear combination of the random variables, and does not have any physical significance with respect to the failure probability of the structure.

3.2.2. Sequential optimization and reliability assessment (SORA) for RBTO

By using SORA, the RBTO model is decoupled into sequential cycles of equivalent deterministic topology optimization, followed by confirmation of the reliability analysis[25]. In each cycle, the equivalent deterministic topology optimization formulation is updated based on the MPP information obtained from the reliability analysis of the previous cycle. The entire optimization process is repeated until the deterministic topology optimization becomes convergent and the reliability requirements are satisfied. The SORA for RBTO can be expressed as

$$\begin{aligned} \min_{\boldsymbol{\rho}}: \ & C\left(\boldsymbol{\rho}^{(k)}\right) \\ s.t.: \ & \begin{cases} G_i\left(\boldsymbol{\rho}^{(k)}, \boldsymbol{x}_i^{(k-1)}\right) \geq 0 \quad (i=1,\ldots,m) \\ \boldsymbol{\rho}_{\min} \leq \boldsymbol{\rho}^{(k)} \leq \boldsymbol{\rho}_{\max} \end{cases} \end{aligned} \tag{15}$$

where k indicates the end cycle of each deterministic topology optimization; $\boldsymbol{x}_i^{k-1}$ is the MPP vector in the physical space with respect to the ith limit state in the $(k-1)$th cycle, given by the transformation of $\boldsymbol{u}_i^{*(k-1)}$. Provided the current optimal design $\boldsymbol{\rho}^{*(k)}$, the next MPP $\boldsymbol{u}_i^{*(k)}$ can be obtained via the PMA analysis, defined as

$$\begin{aligned} \min_{\boldsymbol{u}}: \ & g_i\left(\boldsymbol{\rho}^{*(k)}, \boldsymbol{u}\right) \\ s.t.: \ & \|\boldsymbol{u}\| = \sqrt{\boldsymbol{u}^{\mathrm{T}}\boldsymbol{u}} = \beta_i^T \end{aligned} \tag{16}$$

Through this decoupling method procedure, the number of reliability analyses can be significantly reduced as it is equal to the number of cycles. Therefore, the computational efficiency can be much higher than the double-loop approach. What's more, it can be easily implemented via the integration with any traditional topology optimization software.

IV. Structural Reliability Analysis

In practice, when using the FORM, the RBTO requires explicit formulation of the limit state function. However, in many complex structures, relationships between the output responses and the input data usually do not exist, especially when applications of numerical methods such as the finite element analysis are involved. Therefore, the metamodeling-based approaches are generally suggested in constructing the unknown limit state function explicitly, making it convenient to use the FORM directly. When applying the metamodeling techniques to the structural reliability analysis, two key issues should be focused on, i.e. the construction of accurate metamodeling approximations and the design of experiments.

4.1. Stochastic response surface method

The stochastic response surface method (SRSM) is one of the most widely used meta-modeling techniques in reliability analysis[26,27], which extends the classical deterministic response surface methodology to structures with uncertain inputs and response outputs. By means of the SRSM, the implicit limit state function is approximated through a series of expansions consisting of the multi-dimensional Hermite orthogonal polynomials of independent normalized random variables with undetermined coefficients, given as

$$g(\boldsymbol{u}) = a_0\Gamma_0 + \sum_{i_1=1}^{d} a_{i_1}\Gamma_1(u_{i_1}) + \sum_{i_1=1}^{d}\sum_{i_2=1}^{i_1} a_{i_1 i_2}\Gamma_2(u_{i_1}, u_{i_2}) + \sum_{i_1=1}^{d}\sum_{i_2=1}^{i_1}\sum_{i_3=1}^{i_2} a_{i_1 i_2 i_3}\Gamma_3(u_{i_1}, u_{i_2}, u_{i_3}) + \cdots \tag{17}$$

where $\{u_i\}_{i=1}^{\infty}$ is a set of independent normalized random variables; a_0, $a_{i1}, \ldots$, are deterministic coefficients to be estimated; $g(\boldsymbol{u})$ is the approximated limit state function; and Γ_i are the Hermite polynomials of degree p. For example, a two dimensional SRSM with second order can be expressed as

$$g(\boldsymbol{u}) = a_0 + a_1u_1 + a_2u_2 + a_3\left(u_1^2 - 1\right) + a_4(u_1u_2) + a_5\left(u_2^2 - 1\right) \tag{18}$$

Based on a set of sampling points N and the corresponding real function evaluations $\bar{g}(\boldsymbol{u})$, the coefficients a_i can be estimated by minimizing the following residual error function:

$$\min\ J(\boldsymbol{a}) = \sum_{i=1}^{N}\varepsilon_i^2 = \sum_{i=1}^{N}\left(\bar{g}(u_i) - g(u_i)\right)^2 \tag{19}$$

Applying the least square method, the analytical solution can be obtained via the matrix approach as follows:

$$\boldsymbol{a} = \left(\boldsymbol{\Gamma}^{\mathrm{T}}\boldsymbol{\Gamma}\right)^{-1}\boldsymbol{\Gamma}^{\mathrm{T}}\bar{\boldsymbol{g}} \tag{20}$$

where $\bar{\boldsymbol{g}}$ is the vector of limit state functions at sampling points; and $\boldsymbol{\Gamma}$ is the matrix of bases at sampling points, defined as

$$\boldsymbol{\Gamma a} = \bar{\boldsymbol{g}} \Rightarrow \begin{bmatrix} \Gamma_0(u_1) & \Gamma_1(u_1) & \cdots & \Gamma_P(u_1) \\ \Gamma_0(u_2) & \Gamma_1(u_2) & \cdots & \Gamma_P(u_2) \\ \vdots & \vdots & \ddots & \vdots \\ \Gamma_0(u_N) & \Gamma_1(u_N) & \cdots & \Gamma_P(u_N) \end{bmatrix} \begin{Bmatrix} a_0 \\ a_1 \\ \vdots \\ a_P \end{Bmatrix} = \begin{Bmatrix} \bar{g}(u_1) \\ \bar{g}(u_2) \\ \vdots \\ \bar{g}(u_N) \end{Bmatrix} \tag{21}$$

where $(P+1)$ is the number of bases. In order to achieve rapid convergence with an acceptable level of accuracy being maintained, the design of experiment (DOE) to generate suitable sampling points becomes an important issue in the SRSM.

4.2. Sparse grid method

The sparse grid method is a special discretization technique, which can be traced back to the Smolyak algorithm[28]. It is based on the hierarchical basis, which is a representation of a discrete function space equivalent to the conventional nodal basis, and a sparse tensor product construction[29]. Compared with the support nodes obtained via a 'full grid' algorithm, much less scenarios are constructed through the use of a certain combination of special tensor products in the Smolyak algorithm. The readers are referred to the paper by Xiong[30] and the references therein for more information. In this study, the sparse grid method was proposed to generate sampling points for the SRSM construction, which provided an attractive experimental design scheme.

Let U_1^i denote the one-dimension support nodes, which can be obtained using the univariate quadrature algorithms, such as the Newton-Cotes, Gauss quadrature, Clenshaw-Curtis rules[31], etc. Thus the d-dimensional sampling points $\boldsymbol{U}_d$ with k levels ($k \geq 0$) generated by the Smolyak algorithm, a tensor product rule specific to spares grids, are given as:

$$\boldsymbol{U}_d^k = \bigcup_{q-d+1 \leq |\boldsymbol{i}| \leq q} \left(U^{i_1} \otimes \cdots \otimes U^{i_d}\right) \tag{22}$$

where $q = k + d$; and $|\boldsymbol{i}|$ denotes the summation of multi-indices ($|\boldsymbol{i}| = i_1 + \ldots + i_d$) which is intelligently bounded such that the tensor products can exclude the points from full grids without losing the approximation accuracy.

In this paper, the Chebyshev-Gauss-Lobatto type sparse grid H^{CC} is constructed[32]. Here, the support points u_j^i comprising the set of support nodes $\boldsymbol{U}^i = \{u_1^i, \ldots, u_d^i\}$ are defined as

$$u_j^i = \begin{cases} \dfrac{-\cos\left[\pi (j-1) / (m_i - 1)\right] + 1}{2} & \text{for} \quad j = 1, \cdots, m_i, \quad \text{if} \quad m_i > 1 \\ 0.5 & \text{if} \quad m_i = 1 \end{cases} \tag{23}$$

where, $m_i = \begin{cases} 1 & \text{if} \quad i = 1 \\ 2^{i-1} + 1 & \text{if} \quad i > 1 \end{cases}$

Examples of the two- and three-dimensional support nodes of Smolyak sparse grid based on the Chebyshev-Gauss-Lobatto rule with level $l = 2$ are shown in Fig.2.

V. Numerical Examples

In this section, three examples are demonstrated by comparing the results obtained using the DTO with those using the RBTO, including the double-loop formulations (PMA), and the decoupled approaches (Hybrid and SORA). The standard SIMP method has been implemented in a MATLAB setting for all these numerical examples, which are solved using the method of moving Asymptotes (MMA) with standard settings[33]. To ensure the existence of solutions, the basic mesh-independent density filtering is used to eliminate the appearance of numerical instabilities[34], such as the checkerboard pattern and mesh dependency. The procedure of topology optimization is conducted on a Window 7 workstation (Intel Xeon (R) E5440, 2.83GHz, 4.00GB RAM, 8 cores).

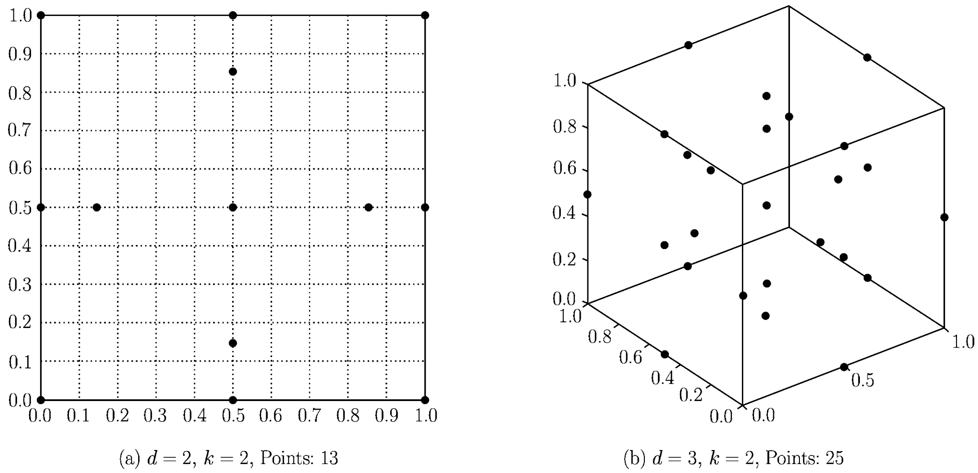

Fig. 2. The Chebyshev-Gauss-Lobatto type sparse grid.

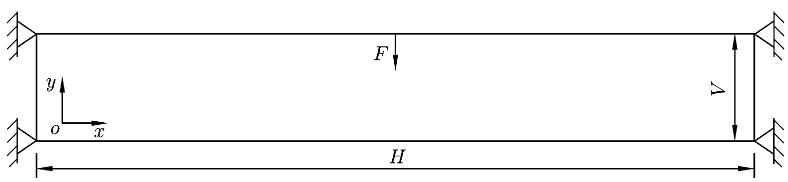

Fig. 3. Design domain and loading conditions.

Table 1. **Geometrical and material properties and loading condition, uncertainties marked by mean values**

Geometry	Horizontal length	$H = 100$ mm
	Vertical length	$V = 15$ mm
	Thickness	$t = 1$ mm
Material property	Young's modulus	$E_0 = 7.1 \times 10^4$ MPa
	Poisson's ratio	$\nu = 0.33$
Loading condition	External load	$F = 100$ N

5.1. A simple supported beam

In the first example, a simple supported beam with a single load case, as shown in Fig.3, was optimized to minimize the volume fraction under a vertical displacement constraint being enforced at the loading point. The geometrical and material properties, as well as the loading condition are listed in Table 1. The design domain was discretized by 1500 (100×15) four-node bi-linear finite elements.

The selected two random variables were Young's modulus E_0 and the magnitude of external load F, which were assumed to obey normal distributions with a variance of 5% from the mean values. The limit state function was defined as $G = \delta_{\max} - \delta$ with δ being the actual vertical displacement and $\delta_{\max}$ the maximum allowable displacement assigned as 0.142 mm. The target reliability index was assumed to be 3.0 for displacement constraint.

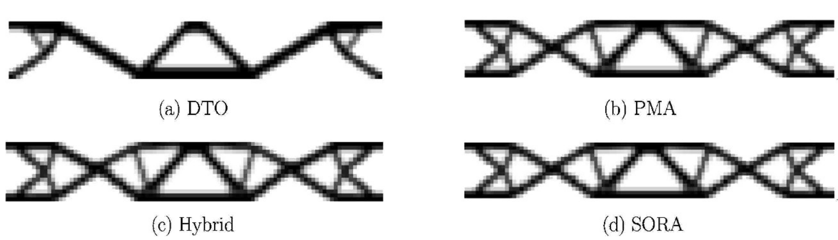

Fig. 4. Optimized design obtained from various approaches.

Table 2. **Comparison of topology optimization design results**

Approach		Volume fraction (%)	Reliability index (β)	Computing time (s)	Design point	
					E_0 (MPa)	F (N)
DTO		30.87	1.5426×10^{-5}	28.89	-	-
RBTO	PMA	40.37	3.000	143.98	6.28×10^{4}	109.61
	Hybrid	40.27	2.9687	39.31	6.49×10^{4}	108.66
	SORA	40.37	3.000	49.50	6.28×10^{4}	109.61

Table 3. **Approximated limit state function constructed by SRSM in PMA**

Iteration	a_0	a_1	a_2	a_3	a_4	a_5
1	−1.4673	0.1257	−0.1247	−0.0063	0.0063	−0.0000
2	−0.2534	0.0638	−0.0633	−0.0032	0.0032	−0.0000
⋮	⋮	⋮	⋮	⋮	⋮	⋮
53	0.1907	0.0412	−0.0409	−0.0021	0.0021	−0.0000
54	0.1907	0.0412	−0.0409	−0.0021	0.0021	−0.0000

Approximated limit state function:
$g(\boldsymbol{u}) = a_0 + a_1u_1 + a_2u_2 + a_3(u_1^2 - 1) + a_4u_1u_2 + a_5(u_2^2 - 1)$

Table 4. **Approximated limit state function constructed by SRSM in SORA**

Iteration	a_0	a_1	a_2	a_3	a_4	a_5
1	−0.0026	0.0511	−0.0507	−0.0026	0.0026	−0.0000
2	0.1907	0.0412	−0.0409	−0.0021	0.0021	−0.0000

The optimal topologies are presented in Fig.4, with the corresponding results summarized in Table 2, including volume fraction, reliability index, computing time and design point. The reliability index was calculated using the standard 100,000 Monte Carlo simulations. The coefficients of SRSM at some iteration during the PMA and SORA procedures are given in Tables 3 and 4, respectively, where u_1 and u_2 are the normalized values of E_0 and F, respectively.

5.2. An L-shaped structure

In this example, an L-shaped structure with two load cases, shown in Fig.5, was optimized to minimize the volume fraction under the compliance constraint. The geometrical and material properties, as well as the loading conditions are summarized in Table 5. The design domain was meshed with 3600 (60×60) four-node elements.

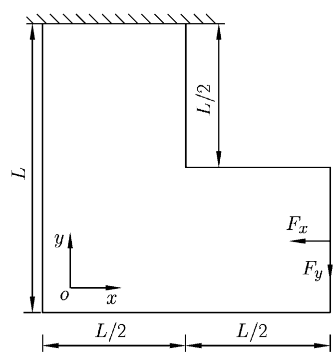

Fig. 5. Design domain and boundary conditions.

The three random variables were selected as Young's modulus E_0 and the magnitudes of external loads F_x and F_y, which were assumed to follow normal distributions with a variance of 5% from the mean values. The limit state function was defined as $G = c_{\max} - c$, with c being the sum of compliance associated with the two load cases and $c_{\max}$ the maximum allowable compliance assigned as 40 N·mm. The target reliability index was assumed to be 3.0 for compliance constraint.

Table 5. **Geometrical and material properties and loading conditions, uncertainties marked by mean values**

Geometry	Length	$L = 60$ mm
	Thickness	$t = 1$ mm
Material property	Young's modulus	$E_0 = 7.1 \times 10^4$ MPa
	Poisson's ratio	$\nu = 0.33$
Loading conditions	Load case I	$F_x = 150$ N
	Load case II	$F_y = 100$ N

In Fig.6, the optimal topologies are shown, with the results summarized in Table 6, including volume fraction, reliability index, computing time and design point. The reliability index was calculated using the standard Monte Carlo simulations. The coefficient of SRSM during the PMA and SORA procedures at some iteration are given in Tables 7 and 8, respectively, where u_1, u_2 and u_3 are the normalized values of E_0, F_x and F_y, respectively.

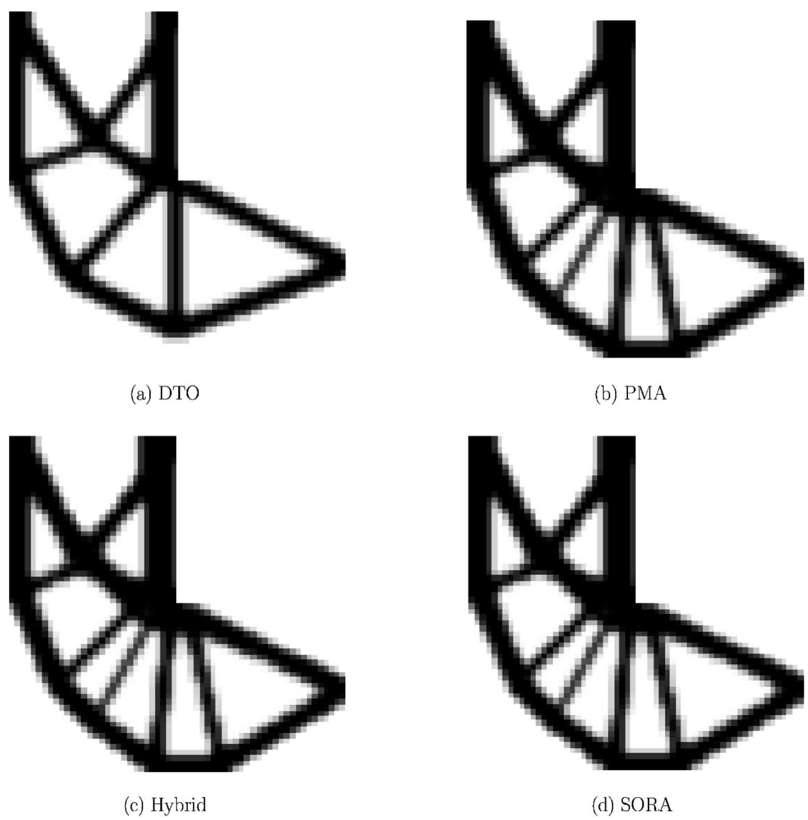

Fig. 6. Optimized design obtained from various approaches.

Table 6. **Comparison of topology optimization design results**

Approach		Volume fraction (%)	Reliability index (β)	Computing time (s)	Design point E_0 (MPa)	F_x (N)	F_y (N)
DTO		25.52	1.7801×10^{-5}	960.78	-	-	-
RBTO	PMA	32.09	3.000	3431.23	6.42×10^4	162.79	107.79
	Hybrid	32.07	2.9725	158.20	6.49×10^4	162.99	108.66
	SORA	32.09	3.000	1509.29	6.42×10^4	162.79	107.79

Table 7. **Approximated limit state function constructed by SRSM in PMA**

Iteration	a_0	a_1	a_2	a_3	a_4	a_5	a_6	a_7	a_8	a_9
1	−1.8709	0.1472	−0.1404	−0.1476	−0.0074	0.0071	−0.0035	0.0000	−0.0037	0.0075
2	−0.3074	0.0670	−0.0581	−0.0730	−0.0034	0.0029	−0.0015	0.0000	−0.0018	0.0037
⋮	⋮	⋮	⋮	⋮	⋮	⋮	⋮	⋮	⋮	⋮
73	0.2234	0.0398	−0.0373	−0.0406	−0.0020	0.0019	−0.0009	0.0000	−0.0010	0.0021
74	0.2234	0.0398	−0.0373	−0.0406	−0.0020	0.0019	−0.0009	0.0000	−0.0010	0.0021

Approximated limit state function:

$$g(\boldsymbol{u}) = a_0 + a_1u_1 + a_2u_2 + a_3u_3 + a_4(u_1^2 - 1) + a_5u_1u_2 + a_6(u_2^2 - 1) + a_7u_2u_3 + a_8(u_3^2 - 1) + a_9u_1u_3$$

Table 8. **Approximated limit state function constructed by SRSM in SORA**

Iteration	a_0	a_1	a_2	a_3	a_4	a_5	a_6	a_7	a_8	a_9
1	−0.0050	0.0515	−0.0473	−0.0536	−0.0026	0.0024	−0.0012	0.0000	−0.0013	0.0027
2	0.2233	0.0398	−0.0375	−0.0405	−0.0020	0.0019	−0.0009	−0.0000	−0.0010	0.0021
3	0.2234	0.0398	−0.0373	−0.0406	−0.0020	0.0019	−0.0009	−0.0000	−0.0010	0.0021

5.3. A multiple load bridge problem

A multiple load bridge problem as shown in Fig.7 was optimized to minimize the volume fraction under the compliance constraint. The geometrical and material properties, as well as the loading conditions are summarized in Table 9. Three load cases were considered here. The design domain was meshed with 5400 (90×60) four-node elements.

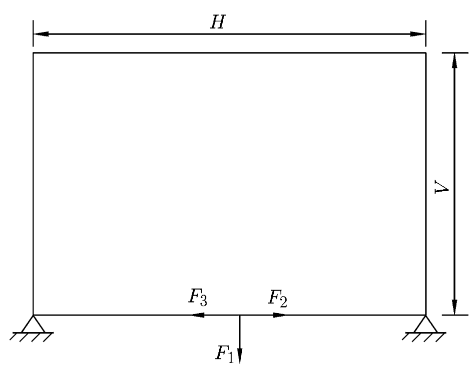

Fig. 7. Design domain and boundary conditions.

Table 9. **Geometrical and material properties and loading conditions, uncertainties marked by mean values**

Geometry	Horizontal length	$H = 90$ mm
	Vertical length	$V = 60$ mm
	Thickness	$t = 1$ mm
Material property	Young's modulus	$E_0 = 7.1 \times 10^4$ MPa
	Poisson's ratio	$\nu = 0.33$
Loading condition	Load case I	$F_1 = 100$ N
	Load case II	$F_2 = 100$ N
	Load case III	$F_3 = 100$ N

The selected four random variables were Young's modulus E_0 and the magnitudes of loads F_1, F_2, F_3, which were assumed to follow normal distributions with a variance of 10% from the mean values. The limit state function was defined as $G = c_{\max} - c$, with c being the sum of compliance for the three load cases and $c_{\max}$ the maximum allowable compliance assigned as 7 N·mm. The target reliability index was assumed to be 3.0 for compliance constraint.

The optimal topologies are shown in Fig.8, and the corresponding results are compared in Table 10, including volume fraction, reliability index, computing time and design point. The reliability index was calculated using the Monte Carlo simulations. And the coefficient of SRSM at some iteration during the PMA and SORA procedures are given in Tables 11 and 12, respectively, where u_1, u_2, u_3 and u_4 are the normalized values of E_0, F_1, F_2 and F_3, respectively.

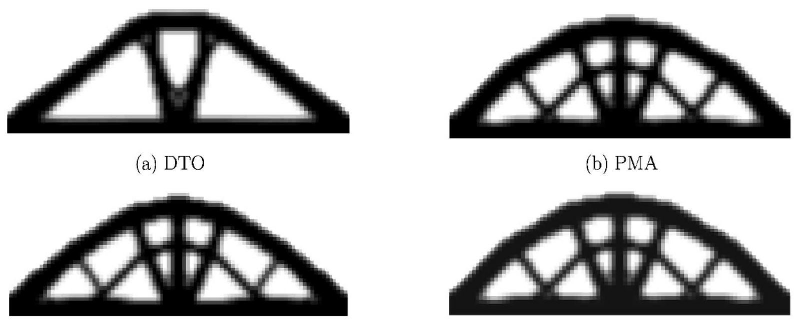

(a) DTO (b) PMA (c) Hybrid (d) SORA

Fig. 8. Optimized design obtained from various approaches.

Table 10. **Comparison of topology optimization design results**

Approach		Volume fraction (%)	Reliability index (β)	Computing time (min)	Design point			
					E_0 (MPa)	F_1 (N)	F_2 (N)	F_3 (N)
DTO		20.12	2.0201×10^{-5}	31.91	-	-		-
RBTO	PMA	25.42	3.000	662.22	5.51×10^4	115.83	108.61	108.61
	Hybrid	24.42	2.9503	35.84	5.87×10^4	117.32	117.32	117.32
	SORA	25.42	3.000	147.16	5.51×10^4	115.83	108.61	108.61

Table 11. **Approximated limit state function constructed by SRSM in PMA**

Iteration	a_0	a_1	a_2	a_3	a_4	a_5	a_6	a_7	a_8
1	−2.6915	0.4058	−0.2344	−0.2541	−0.2541	−0.0409	0.0251	−0.0117	−0.0000
2	−0.5993	0.1758	−0.1635	−0.0791	−0.0791	−0.0177	0.0175	−0.0082	−0.0000
⋮	⋮	⋮	⋮	⋮	⋮	⋮	⋮	⋮	⋮
154	0.1610	0.0922	−0.0786	−0.0451	−0.0451	−0.0093	0.0084	−0.0039	0.0000
155	0.1610	0.0922	−0.0786	−0.0451	−0.0451	−0.0093	0.0084	−0.0039	0.0000
Iteration	a_9	a_{10}	a_{11}	a_{12}	a_{13}	a_{14}			
1	−0.0127	−0.0000	−0.0127	0.0272	0.0272	−0.0000			
2	−0.0039	0.0000	−0.0039	0.0085	0.0085	−0.0000			
⋮	⋮	⋮	⋮	⋮	⋮	⋮			
154	−0.0022	−0.0000	−0.0022	0.0048	0.0048	0.0000			
155	−0.0022	−0.0000	−0.0022	0.0048	0.0048	0.0000			

Approximated limit state function:

$$g(\boldsymbol{u}) = a_0 + a_1u_1 + a_2u_2 + a_3u_3 + a_4u_4 + a_5(u_1^2 - 1) + a_6u_1u_2 + a_7(u_2^2 - 1) + a_8u_2u_3 + a_9(a_3^2 - 1) + a_{10}u_3u_4 + a_{11}(u_4^2 - 1) + a_{12}u_1u_4 + a_{13}u_1u_3 + a_{14}u_2u_4$$

5.4. Comparative performances of the three RBTO approaches

From the comparison of the results, the DTO yields optimal topologies with low reliability levels, where uncertainties are not taken into account. For the RBTO, more volume material is required to achieve the target reliability index; and by comparison with the DTO, a distinct difference in topology

Table 12. **Approximated limit state function constructed by SRSM in SORA**

Iteration	a_0	a_1	a_2	a_3	a_4	a_5	a_6	a_7	a_8
1	−0.0204	0.1122	−0.1009	−0.0522	−0.0522	−0.0113	0.0108	−0.0051	−0.0000
2	0.1550	0.0929	−0.0798	−0.0451	−0.0451	−0.0094	0.0085	−0.0040	−0.0000
3	0.1512	0.0933	−0.0794	−0.0457	−0.0457	−0.0094	0.0085	−0.0040	−0.0000
4	0.1610	0.0922	−0.0786	−0.0451	−0.0451	−0.0093	0.0084	−0.0039	0.0000
Iteration	a_9	a_{10}	a_{11}	a_{12}	a_{13}	a_{14}			
1	−0.0026	−0.0000	−0.0026	0.0056	0.0056	−0.0000			
2	−0.0022	0.0000	−0.0022	0.0048	0.0048	−0.0000			
3	−0.0023	−0.0000	−0.0023	0.0049	0.0049	−0.0000			
4	−0.0022	−0.0000	−0.0022	0.0048	0.0048	0.0000			

configuration may emerge, which can be found in all the three examples. In the example of the simple supported beam, the reliability level for the optimum of DTO is nearly 0, and the RBTO uses up to about 9% more material in design domain than the DTO to achieve the target reliability level. It is also observed that higher computation cost is required by the RBTO due to the reliability analysis on exploring the design point, especially for the PMA and SORA, meaning that reliability enhancement is inevitably accompanied with the sacrifice of computational expense. It can be demonstrated that the reliability concept is necessary to be incorporated into the topology optimization when considering the uncertainties, such as external loads and material properties.

Results obtained from the three examples have demonstrated that the three typical RBTO approaches have similar optimal topologies. This is not surprising because the proposed methods are all implemented based on the reliability theory. For comparison purpose, there exists a considerable difference in computational costs, which is mainly dependent on the number of reliability analyses. The computational effort for PMA is very high due to the multiplication of the iteration numbers in both topology optimization and reliability analysis loops. The reliability analysis for SORA is only conducted after the equivalent topology optimization procedure, which is equal to the number of the entire cycles. However, the Hybrid only has one reliability analysis loop at the beginning of the procedure where the limit state function is predetermined as a linear combination of the random variables. Therefore, the Hybrid is more efficient than the PMA and SORA. But the PMA and SORA are superior to the Hybrid in view of the computational accuracy, for the Hybrid does not have any physical significance with respect to the failure probability of the structure. It can be seen from the L-shaped structure problem that, computing time for the SORA is 1509.29 s corresponding to the number of reliability analyses being significantly reduced to 3, compared with that of up to 3431.23 s with 171 times of reliability analysis for the PMA. Especially, the Hybrid is even more efficient than the DTO when the reliability analysis is excluded from the entire RBTO procedure for auxiliary implementation. It is also demonstrated from the results that the reliability level of the Hybrid is slightly lower than those of the PMA and SORA reaching up to 3.0 through the validation using Monte Carlo Simulation.

Results presented herein have also shown that, the SRSM with sparse grid method is capable of producing an efficient reliability analysis in the RBTO, where the limit state function is approximated using the SRSM, and the reasonable sampling points for the design of experiments are generated using the sparse grid method. For the example of the multiple load bridge problem, the limit state function involving the relationship between the structural compliance and uncertainty parameters are clearly exhibited during the PMA and SORA procedures. It can be clearly observed that the final coefficients of SRSM for the PMA and SORA have the same values in the construction of the limit state function, exploring the identical design points.

VI. Conclusion

This paper integrates the reliability concept into the SIMP-based topology optimization to solve the RBTO problems. Specifically, three selected typical RBTO methodologies are implemented, discussed and tested upon three numerical examples, including the double-loop formulation (PMA) and the decoupled approaches (Hybrid and SORA). The meta-modeling technique is proposed to construct the implicit limit state function for reliability analysis. From the comparison of the numerical results, the following conclusions are drawn:

(1) The optimal topologies obtained using the proposed RBTO methods are more reliable than that using the DTO; and the RBTO may exhibit manifest differences in topologies. It is demonstrated that the reliability concept is necessary to be integrated into the topology optimization when taking into account the effect of uncertainty parameters such as material properties and external loads.

(2) The double loop approach (PMA) is easy to implement, but the computational cost is unaffordable for complex structures due to the multiplication of the iteration numbers in both topology optimization and reliability analysis loops. Although specific treatment is required, the decoupled approaches (Hybrid and SORA) are recommended for their efficiency and small loss of accuracy.

(3) The SRSM combined with the sparse grid method can be used to conduct an efficient reliability analysis for the RBTO, where the limit state function is explicitly approximated by the SRSM through a series of expansions consisting of the multi-dimensional Hermite orthogonal polynomials with the design of experiments generated using the sparse grid method.

(4) Future research on implementation and testing of the proposed RBTO methods is still suggested. One possible extension includes the design of compliant mechanisms and multi-physics problems. Another interesting point of possibility is applications of various metamodeling methods in the RBTO, such as the Kriging and support vector machine.

References

[1] Bendsøe,M.P. and Kikuchi,N., Generating optimal topologies in structural design using a homogenization method. *Computer Methods in Applied Mechanics and Engineering*, 1988, 71(2): 197-224.

[2] Bendsøe,M.P. and Sigmund,O., Topology Optimization: Theory, Methods and Applications. Berlin: Springer-Verlag Berlin Heidelberg Company, 2003.

[3] Chen,C.Y., Pan,J. and Wang,D.Y., The satellite structure topology optimization based on homogenization method and its size sensitivity analysis. *Acta Mechanica Solida Sinica*, 2005, 18(2): 173-180.

[4] Lee,J.O., Yang,Y.S. and Ruy,W.S., A comparative study on reliability-index and target-performance-based probabilistic structural design optimization. *Computers & Structures*, 2002, 80(3-4): 257-269.

[5] Maute,K. and Frangopol,D.M., Reliability-based design of MEMS mechanisms by topology optimization. *Computers & Structures*, 2003, 81(8): 813824.

[6] Kim,C., Wang,S.Y, Bae,K.R., Moon,H. and Choi,K.K., Reliability-based topology optimization with uncertainties. *Journal of Mechanical Science and Technology*, 2006, 20(4): 494-504.

[7] Cho,K.H., Park,J.Y., Im,M.G. and Han,S.Y., Reliability-based topology optimization of electro-thermal-compliant mechanisms with a new material mixing method. *International Journal of Precision Engineering and Manufacturing*, 2012, 13(5): 693-699.

[8] Kharmanda,G., Olhoff,N., Mohamed,A. and Lemaire,M., Reliability-based topology optimization. *Structural and Multidisciplinary Optimization*, 2004, 26(5): 295-307.

[9] Silva,M., Tortorelli,D.A., Norato,J.A., Ha,C. and Bae,H.R., Component and system reliability-based topology optimization using a single-loop method. *Structural and Multidisciplinary Optimization*, 2010, 41(1): 87-106.

[10] Nguyen,T.H., Song,J. and Paulino,G.H., Single-loop system reliability-based topology optimization considering statistical dependence between limit-states. *Structural and Multidisciplinary Optimization*, 2011, 44(5): 593-611.

[11] Yoo,K.S., Eom,Y.S., Park,J.Y., et al., Reliability-based topology optimization using successive standard response surface method. *Finite Elem Anal Des*, 2011, 47(8): 843-849.

[12] Eom,Y.S., Yoo,K.S., Park,J.Y. and Han,S.Y., Reliability-based topology optimization using a standard response surface method for three-dimensional structures. *Structural and Multidisciplinary Optimization*, 2011, 43(2): 287-295.

[13] Suzuki,K. and Kikuchi,N., A homogenization method for shape and topology optimization. *Computer Methods in Applied Mechanics and Engineering*, 1991, 93 (3): 291-318.

[14] Bendsøe,M.P., Optimal shape design as a material distribution problem. *Computers & Structures*, 1989, 1(4): 193-202.

[15] Xie,Y.M. and Steven,G.P., A simple evolutionary procedure for structural optimization. *Computers & Structures*, 1993, 49(5): 885-896.

[16] Wang,M.Y., Wang,X. and Guo,D., A level set method for structural topology optimization. *Computer Methods in Applied Mechanics and Engineering*, 2003, 192(1-2): 227-246.

[17] Eschenauer,H.A. and Olhoff,N., Topology optimization of continuum structures: a review. *Applied Mechanics Reviews*, 2001, 54(4): 331-389.

[18] Lee,S.H. and Chen,W., A comparative study of uncertainty propagation methods for black-box-type problems. *Structural and Multidisciplinary Optimization*, 2009, 37(3): 239-253.

[19] Hasofer,A.M. and Lind,N.C., An exact and invariant first order reliability format. *Journal of Engineering Mechanics—ASCE*, 1974, 100(1): 111-121.

[20] Rosenblatt,M., Remarks on a Multivariate Transformation. *Annals of Mathematical Statistics*, 1952, 23(3): 470-472.

[21] Liu,P.L. and Kiureghian,A.D., Multivariate distribution models with prescribed marginals and covariances. *Probabilistic Engineering Mechanics*, 1986, 1(2): 105-112.

[22] Tu,J. and Choi,K.K., A new study on reliability-based design optimization. *Journal of Mechanical Design-ASME*, 1999, 121(4): 557-564.

[23] Wu,Y.T., Millwater,H.R. and Cruse,T.A., Advanced probabilistic structural analysis method for implicit performance functions. *AIAA Journal*, 1990, 28(9): 1663-1669.

[24] Grujicic,M., Arakere,G., Bell,W.C., Marvi,H., Yalavarthy,H.V., Pandurangan,B., Haque,I. and Fadel,G.M., Reliability-Based Design Optimization for Durability of Ground Vehicle Suspension System Components. *Journal of Materials Engineering and Performance*, 2010, 19(3): 301-313.

[25] Du,X. and Chen,W., Sequential optimization and reliability assessment method for efficient probabilistic design. *Journal of Mechanical Design-ASME*, 2004, 126(2): 225-233.

[26] Isukapalli,S.S., Roy,A. and Georgopoulos,P.G., Stochastic response surface methods (SRSMs) for uncertainty propagation: application to environmental and biological systems. *Risk Analysis*, 1998, 18(3): 351-363.

[27] Xiong,F.F., Chen,W., Xiong,Y. and Yang,S., Weighted stochastic response surface method considering sample weights. *Structural and Multidisciplinary Optimization*, 2011, 43(6): 837-849.

[28] Smolyak,S.A., Quadrature and interpolation formulas for tensor products of certain classes of functions. *Doklady Akademii nauk SSSR*, 1963, 1(4): 240-243.

[29] Yserentant,H., On the multi-level splitting of finite element spaces. *Numerische Mathematik*, 1986, 49(4): 379-412.

[30] Xiong,F.F., Greene,S., Chen,W., Xiong,Y. and Yang,S.X., A new sparse grid based method for uncertainty propagation. *Structural and Multidisciplinary Optimization*, 2010, 41(3): 335-349.

[31] Gerstner,T. and Griebel,M., Numerical integration using sparse grids. *Numerical Algorithms*, 1998, 18(3-4): 209-232.

[32] Clenshaw,C.W. and Curtis,A.R., A method for numerical integration on an automatic computer. *Numerische Mathematik*, 1960, 2(1): 197-205.

[33] Svanberg,K., The method of moving asymptotes-a new method for structural optimization. *International Journal for Numerical Methods in Engineering*, 1987, 24(2): 359-373.

[34] Sigmund,O., Morphology-based black and white filters for topology optimization. *Structural and Multidisciplinary Optimization*, 2007, 33(4-5): 401-424.